Plant Biotechnology 31, 555–559 (2014)
DOI: 10.5511/plantbiotechnology.14.0908a

Short Communication

Isolation of anthocyanin 7-*O*-glucosyltransferase from Canterbury bells (*Campanula medium*)

Taira Miyahara*, Tomonori Tani, Mariko Takahashi, Yuzo Nishizaki, Yoshihiro Ozeki, Nobuhiro Sasaki[a]

Department of Biotechnology and Life Science, Tokyo University of Agriculture and Technology, Koganei, Tokyo 184-8588, Japan
* E-mail: miyahara@cc.tuat.ac.jp Tel & Fax: +81-42-388-7386

Received June 24, 2014; accepted September 8, 2014 (Edited by A. Sugiyama)

Abstract Canterbury bells (*Campanula medium*) have deep purple petals due to the accumulation of 7-polyacylated anthocyanin molecules. The first step in the production of 7-polyacylated anthocyanins is glucosylation at the C7 position of anthocyanidin mediated by an acyl-glucose dependent anthocyanin 7-*O*-glucosyltransferase (AA7GT). To date, two such enzymes have been identified: DgAA7GT from delphinium (*Delphinium grandiflorum*) and AaAA7GT from African lily (*Agapanthus africanus*). Here, we describe the isolation of AA7GT cDNA from *C. medium* and the characterization of the enzymatic properties of a recombinant protein. The CmAA7GT protein belongs to glycoside hydrolase family 1, similarly to other AA7GTs; a phylogenetic analysis revealed that CmAA7GT was in the same clade as other AA7GTs. The *CmAA7GT* gene showed expression only in flowers, with a peak level of expression at the middle stage of floral development. A recombinant CmAA7GT protein showed significant preference for interaction with anthocyanidin 3-*O*-rutinoside rather than anthocyanidin 3-*O*-monoglycoside, which is the preferred target of other AA7GTs. This difference in target preference may reflect a conformational difference in the acceptor pocket of the enzyme protein that recognizes the anthocyanidin glycoside.

Key words: Acyl-glucose, anthocyanin 7-*O*-glucosyltransferase, *Campanula medium*, Canterbury bells.

Canterbury bells (*Campanula medium*) is a popular ornamental flower with bell-shaped petals that vary in color from white through pink to purple. Previous studies of pigments in flowers of *C. medium* showed that the major anthocyanin molecule in purple petals is delphinidin 3-*O*-rutinoside-7-*O*-[6-*O*-(4-{6-*O*-[4-(6-*O*-*p*-hydroxybenzoyl-glucosyl)benzoyl]-glucosyl}benzoyl)-glucoside], termed campanin (Supplementary Figure 1; Terahara et al. 1990). The violet flowers of *Delphinium hybridum* accumulate a 7-polyacylated anthocyanin, consisting of two molecules of *p*-hydroxybenzoic acid; this anthocyanin is similar to campanin (Kondo et al. 1990). Blue flowers of other species also accumulate 7-polyacylated anthocyanins (Honda and Saito 2002; Saito et al. 2007); the conformation of these molecules contribute to the intramolecular stacking that causes a bathochromic shift leading to blue coloration (Yoshida et al. 2009). Recent studies on anthocyanins confirmed the importance of hydroxylation of the B-ring of anthocyanidin and also found that anthocyanidin modifications have a significant effect on variations in color depth and production of a blue tone. Although anthocyanin glycosylation is generally catalyzed by an UDP-sugar dependent glycosyltransferase (UGT), to date, there have been no reports on anthocyanin 7-*O*-glycosylation by UGT (Yonekura-Sakakibara et al. 2009). Our previous studies indicated that anthocyanin 7-*O*-glucosyltransferases belong to the glycoside hydrolase family 1 (GH1) and that they utilize acyl-glucose as a glucosyl donor molecule. As a consequence, they are termed acyl-glucose dependent anthocyanin 7-*O*-glucosyltransferases (AA7GTs). These enzymes act through a different catalytic mechanism in the vacuole from that of UGTs in the cytosol. Previously, we identified AA7GTs in the blue sepals of delphinium (*D. grandiflorum*) and the purple petals of African lily (*Agapanthus africanus*) (Matsuba et al. 2010; Miyahara et al. 2012). Delphinium is a eudicot that belongs to the Ranunculaceae (Ranunculales), whereas African lily is a monocot that belongs to the Agapanthaceae

Abbreviations: AA7GT, acyl-glucose dependent anthocyanin 7-*O*-glucosyltransferase; EF1α, elongation factor-1α; pHBG, *p*-hydroxybenzoyl-glucose; Dp3R, delphinidin 3-*O*-rutinoside; Dp3R7G, delphinidin 3-*O*-rutinoside-7-*O*-glucoside; GH1, glycoside hydrolase family 1; HPLC, high-performance liquid chromatography; ORF, open reading frame.

[a] Present address: Iwate Biotechnology Research Center, 22-174-4 Narita, Kitakami, Iwate 024-0003, Japan.

This article can be found at http://www.jspcmb.jp/
Published online November 22, 2014

(Asparagales) (The Angiosperm Phylogeny Group 2009). Despite the evolutionary divergence of the two species, a phylogenetic analysis of their AA7GTs showed that both belonged to the same clade (Miyahara et al. 2012). In order to determine whether this apparent conservation of AA7GTs is widespread in the plant kingdom, we analyzed 7-polyacylated anthocyanin production in the core eudicot *C. medium* (Campanulaceae, Asterales). We were particularly interested in whether anthocyanin 7-glucosylation in *C. medium* was catalyzed by a GH1-type glucosyltransferase that might have originated from the same ancestral gene as in delphinium and African lily. Here, we describe the successful detection of AA7GT activity in a crude protein extract prepared from the petals of *C. medium* and the identification of a *C. medium AA7GT* cDNA. We also discuss the phylogenetic relationship of plant AA7GTs.

Crude proteins were extracted from petals of *C. medium* cv. Blue Get Mee, precipitated with ammonium sulfate, and desalted as previously described (Nishizaki et al. 2013). A standard reaction mixture (20 μl) consisted of 3.7 μg of crude protein, 45 nmol *p*-hydroxybenzoyl-glucose (pHBG) and 2 nmol delphinidin 3-*O*-rutinoside (Dp3R) in 1.6 μmol sodium citrate buffer (pH 5.5); the mixture was incubated at 30°C for 1 h. The reaction was terminated by addition of 1.5 μl 20% phosphoric acid and precipitates were removed after centrifugation. The reaction products were analyzed with a high-performance liquid chromatography (HPLC)-photodiode array detector (LaChrom Elite system: Hitachi Hi-Technologies, Tokyo, Japan) equipped with a COSMOSIL 5C18-MS-Packed Column (4.6×50 mm: Nacalai Tesque, Kyoto, Japan) using a linear gradient elution (1.5 ml min^{-1}) of 15 to 60% methanol in 1.5% aqueous phosphoric acid for 5 min.

When the reaction mixture included pHBG as the glucosyl donor, a peak was observed (Figure 1A, arrow) that was absent when the reaction was run without pHBG; in the latter reaction, no significant peaks were detected (Figure 1B). The retention time of the new peak was consistent with that of authentic delphinidin 3-*O*-rutinoside-7-*O*-glucoside (Dp3R7G) (Figure 1E) prepared as described previously (Nishizaki et al. 2013). This analysis confirmed that glucosylation at the 7 position of anthocyanin was catalyzed by an acyl-glucose dependent glucosyltransferase in *C. medium*.

We sought to isolate the *C. medium* (Cm) AA7GT cDNA from total RNA that had been prepared from *C. medium* petals using a RNeasy Plant Mini Kit (Qiagen, Hilden, Germany). Candidate AA7GT cDNAs were obtained using the degenerate primers AAG TdgF and AAG TdgR (Supplementary Table 1) using the 3′-Full RACE Core Set (Takara Bio, Shiga, Japan). The 5′-end of AA7GT cDNA was obtained using the SMARTer RACE cDNA Amplification Kit (Clontech, Mountain

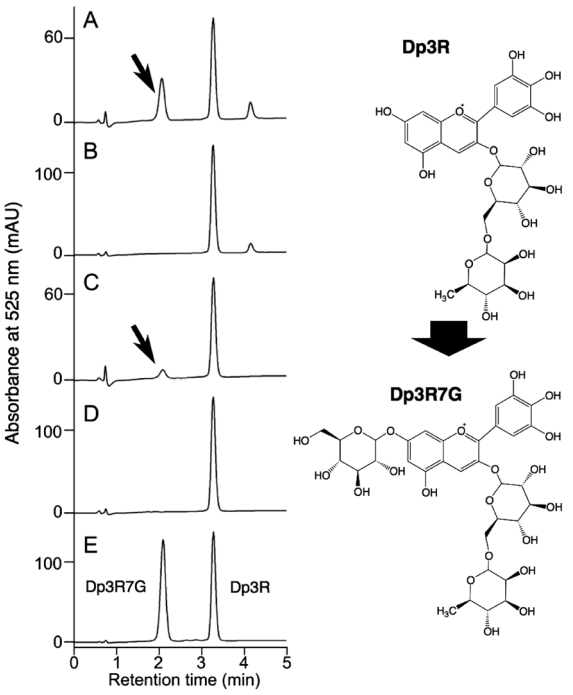

Figure 1. Detection of AA7GT activity using Dp3R as an acceptor. (A) AA7GT assay in the presence of pHBG as a glucosyl donor using a crude protein extract prepared from *C. medium* petals and (B) the same assay in the absence of pHBG. (C) AA7GT assay in the presence of pHBG as the glucosyl donor using a crude extract from recombinant *E. coli* expressing CmAA7GT and (D) the same in the absence of pHBG. (E) Authentic standards of Dp3R and Dp3R7G.

View, CA, USA) according to the manufacturer's protocol and using the Cm7GT5′raceR primer (Supplementary Table 1) and the Universal Primer A Mix. The 3′-end of the AA7GT candidate cDNA was isolated by PCR with the primer Cm7GTatgF (Supplementary Table 1) and a 3′ site Adaptor Primer (Takara Bio). The open reading frame (ORF) of the AA7GT candidate was amplified by PCR with the primer set Cm7GTatgF and Cm7GTstpR. Analysis of the candidate CmAA7GT cDNA using the SignalP program version 4.1 (http://www.cbs.dtu.dk/services/SignalP/) predicted that it had a putative signal peptide to the vacuole at its N-terminus. In a previous study, we found that some AAGTs would not form a recombinant protein carrying the signal peptide; therefore, the sequence corresponding to the putative signal peptide at the N-terminus was deleted for the heterologous expression analysis. We amplified a cDNA fragment using the primer set Cm7GTexpF and Cm7GTrtR (Supplementary Table 1), which was designed to exclude a 30 amino acid sequence of the N-terminus. The amplified product was inserted into the pTrcHis2 vector (Invitrogen, Carlsbad, CA, USA) and then transformed into *Escherichia coli* BL21 (DE3) cells. Recombinant protein was produced using the same conditions as described previously (Miyahara et al. 2012). Crude protein extracted from recombinant *E. coli* was used for analysis of AA7GT activity using the same assay

conditions as described above except for incubation at 30°C for 4 h. Under these conditions, the recombinant protein from the candidate CmAA7GT showed AA7GT activity (Figure 1C).

We performed a quantitative real-time PCR analysis to examine expression of the *CmAA7GT* gene showing AA7GT activity in five different stages of petal development, and in leaves and stems. The *C. medium* housekeeping gene elongation factor-1*α* (*EF1α*) was selected as the control; this gene was isolated using the degenerate primer set described previously (Miyahara et al. 2013). The primer pairs Cm7GTF and Cm7GTR and CmEF1aF and CmEF1aR (Supplementary Table 1) were designed to amplify *CmAA7GT* and *CmEF1α* cDNAs respectively from transcripts. The expression level of each gene was measured by quantitative PCR using the previously described procedure (Miyahara et al. 2012). We found that the highest level of expression of *CmAA7GT* occurred at stage 3 of petal development and the lowest level at stage 5. *CmAA7GT* transcripts were not detectable in leaves or stems (Figure 2). Thus, transcription of *CmAA7GT* was greatest just before flower opening. This pattern of expression has also been found for other AAGTs that are expressed specifically in flower tissues (Matsuba et al. 2010; Miyahara et al. 2012; Nishizaki et al. 2013).

The nucleotide sequence of the ORF of CmAA7GT cDNA (DDBJ accession no. AB968231) consisted of 1,536 bp encoding a predicted 512 amino acid sequence. The deduced amino acid sequence had 82% and 84% similarity to DgAA7GT (AB510758) and AaAA7GT (AB692769), respectively, and 60% identity to both of these sequences. Phylogenetic analysis showed that CmAA7GT was located in the same clade as other AAGTs, DcAA5GT, AaAA7GT, DgAA7GT and AtBGLU10 (Matsuba et al. 2010; Miyahara et al. 2012; Miyahara et al. 2013), but separate to the acyl-glucose dependent glucosyltransferases DgAA7BG-GT1 and DgAA7BG-GT2 that interact with the *p*-hydroxybenzoyl moiety of delphinidin 3-*O*-rutinoside-7-*O*-(6-*O*-(*p*-hydroxybenzoyl)-glucoside) (Nishizaki et al. 2013) (Figure 3). This result indicated that CmAA7GT was likely derived from the same ancestral GH1 as other AA7GTs, DcAA5GT and AtBGLU10. In contrast, DgAA7BG-GT1 and DgAA7BG-GT2 likely originated from a different GH1 and their roles in glycosylation presumably arose through convergent evolution.

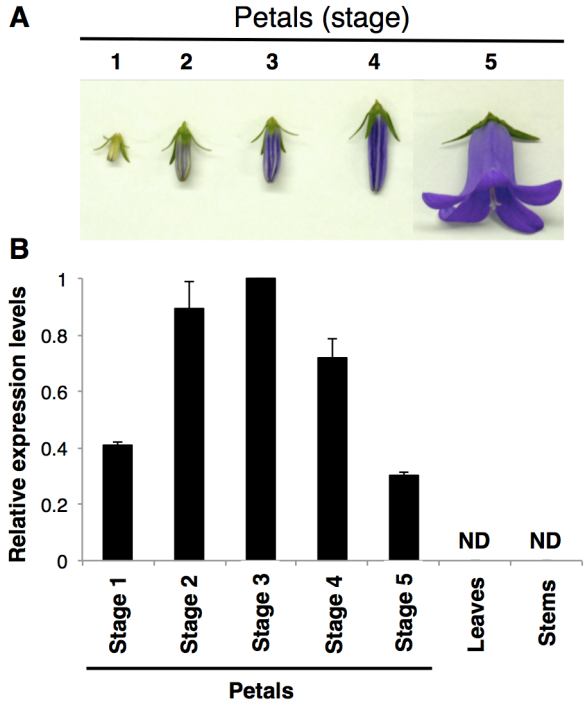

Figure 2. The expression levels of *CmAA7GT* in *C. medium* petals, leaves and stems. (A) Five different petal development stages were examined. (B) The expression levels of *CmAA7GT*. *CmAA7GT* mRNA levels were too low for detection in leaves and stems. ND, not detectable. Error bars indicate ± SD for three biological replicates.

It was difficult to obtain a sufficient amount of purified recombinant CmAA7GT protein because of its low expression level in *E. coli* cells; therefore, we measured the temperature and pH optima of the enzyme and its stability using the partially purified recombinant protein. Crude extracts of the recombinant proteins were filtered through a Millex-GV Syringe Filter Unit (Merck Millipore, Billerica, MA, USA), then applied to a HisTrap HP column (GE Healthcare, Fairfield, CT, USA). The recombinant protein was separated by linear gradient elution (1 ml min^{-1}) using 0 to 100% elution buffer (0.5 M imidazole, 0.5 M NaCl in 0.1 M potassium phosphate buffer, pH 7.5) for 20 min with an Econo Gradient Pump (Bio-Rad, Hercules, CA, USA); 1 ml fractions were collected using a BioLogic BioFrac Fraction Collector (Bio-Rad). The fraction with most CmAA7GT activity was concentrated with 0.1 M citrate buffer (pH 5.5) using an Amicon Ultra-15 (Merck Millipore). Evaluation of the enzymatic properties of CmAA7GT was performed as described previously (Miyahara et al. 2012). The optimum reaction temperature was 35°C and the optimum pH was 6.0. The recombinant protein showed high enzymatic activity across the temperature range 20–40°C for 30 min, and more than 80% activity was retained across a pH range of 6.0 to 9.0 (Supplementary Figure 2). Although this pH range was slightly higher than expected of a vacuolar enzyme, we showed previously that the pH optimum of an AAGT recombinant protein tends to be higher than that of the native protein (Matsuba et al. 2010). This finding indicates that the pH stability of recombinant CmAA7GT might have been shifted to a more alkaline range compared to the native protein. With the exception of a higher stability at alkaline pH, most of the enzymatic properties of CmAA7GT were similar to those described for other AAGTs, DcAA5GT, DgAA7GT, DgAA7BG-

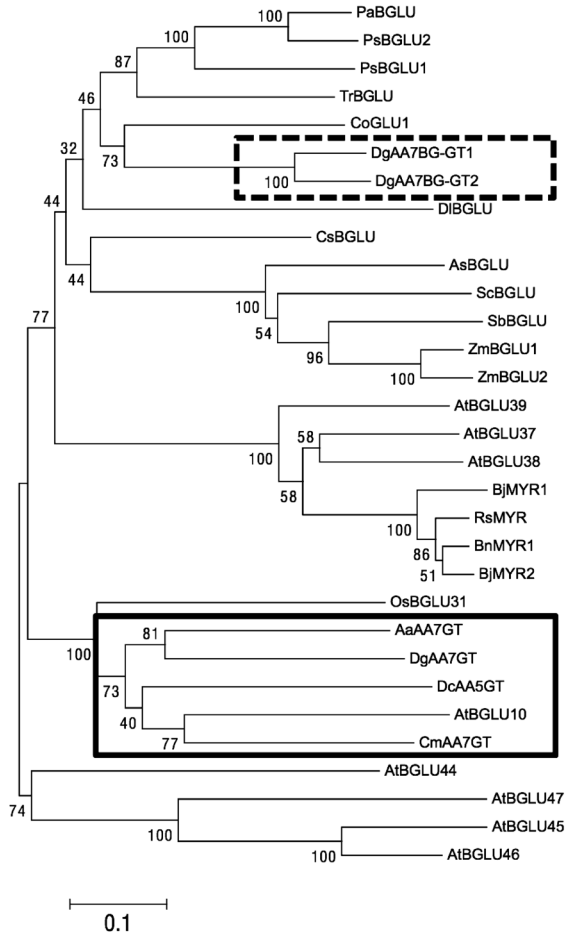

Figure 3. Molecular phylogenetic tree of GH1 members constructed using amino acid sequences. Aa, *Agapanthus africanus* (AaAA7GT: AB692769); As, *Avena sativa* (AsBGLU: X78433); At, *Arabidopsis thaliana* (AtBGLU10: Q93Z14, AtBGLU37: Q9C5C2, AtBGLU38: P37702, AtBGLU39: Q3E8E5, AtBGLU44: Q9LV33, AtBGLU45: O80689, AtBGLU46: O80690, AtBGLU47: Q9SVS1); Bj, *Brassica juncea* (BjMYR1: AY014960, BjMYR2: AJ223494); Bn, *Brassica napus* (BnMYR1: X60214); Cm, *Campanula medium* (CmAA7GT: AB968231); Co, *Consolida orientalis* (CoGLU1: HM559225); Cs, *Costus speciosus* (CsBGLU: D83177); Dc, *Dianthus caryophyllus* (DcAA5GT: AB507446); Dg, *Delphinium grandiflorum* (DgAA7GT: AB510758, DgAA7BG-GT1: AB811444, DgAA7BG-GT2: AB811447); Dl, *Digitalis lanata* (DlBGLU: AJ133406); Os, *Oryza sativa* (OsBGLU31: AK121679); Pa, *Prunus avium* (PaBGLU: U39228); Ps, *Prunus serotina* (PsBGLU1: U26025, PsBGLU2: AF411009); Rs, *Raphanus sativus* (RsMYR: AB042186); Sb, *Sorghum bicolor* (SbBGLU: U33817); Sc, *Secale cereal* (ScBGLU: AF293849); Tr, *Trifolium repens* (TrBGLU: X56733); Zm, *Zea mays* (ZmBGLU1: U44087, ZmBGLU2: U44773). The clade in the box with solid lines includes AAGTs that have been reported by our group, including CmAA7GT reported here. The clade in the box with dashed lines contains the glucosyltransferase to *p*-hydroxybenzoyl moiety of delphinidin 3-*O*-rutinoside-7-*O*-(6-*O*-(*p*-hydroxybenzoyl)-glucoside) (Nishizaki et al. 2013), which is clearly separate from the other AA7GTs. Bar=0.1 amino acid substitutions/site.

GT1, DgAA7BG-GT2 and AaAA7GT (Matsuba et al. 2010; Miyahara et al. 2012; Nishizaki et al. 2013). As the enzymatic reaction proceeded linearly for more than 6 h (data not shown), we selected pH 6.0 and 30°C for 2 h as the assessment conditions to analyze the substrate preferences of CmAA7GT.

Table 1. Donor preferences of recombinant CmAA7GT.

Substrates	Relative activity (%)
Vanillyl-glucose	59.1±1.4
Isovanillyl-glucose	12.3±0.4
p-Hydroxybenzoyl-glucose	72.7±2.9
Sinapoyl-glucose	91.7±0.9
Feruloyl-glucose	98.5±3.9
Caffeoyl-glucose	100±0.0
p-Coumaroyl-glucose	96.2±4.0
Vanillyl-galactose	ND

Analyses of donor preferences were performed with cyanidin 3-*O*-rutinoside as the acceptor. The amount of reaction product was calculated from the area of the HPLC chromatogram recorded at 530 nm. Relative activity is shown in comparison to caffeoyl-glucose which was arbitrarily set as 100%. ND, not detected. All values are means±SD of at least three independent determinations.

Our analyses of substrate preferences indicated that CmAA7GT could utilize various acyl-glucoses molecules, including hydroxycinnamoyl-glucoses (although not isovanillyl-glucose), as the donor substrate (Table 1). This broad donor preference was similar to that of AaAA7GT (Miyahara et al. 2012) but differed from that of DgAA7GT (Matsuba et al. 2010). DgAA7GT shows a preference for C6–C1-glucoses rather than C6–C3-glucoses as a donor. We did not detect accumulation of any acyl-glucoses in *C. medium* petals or in petals of the African lily (data not shown). Thus, it is difficult to speculate which acyl-glucose is utilized by AA7GT as the *in vivo* donor in *C. medium* like the case of African lily. Since campanin has a concatenated *p*-hydroxybenzoyl-glucose structure similar to violdelphin, then *p*-hydroxybenzoyl-glucose might be utilized as a Zwitter donor as described previously for violdelphin biosynthesis (Nishizaki et al. 2013). With regard to CmAA7GT acceptor preference, the number of hydroxyl residues on the anthocyanidin aglycone (two for cyanidin and three for delphinium) had no significant influence on glucosyltransferase activity. However, modification at the 3-position did affect glucosyltransferase activity: a ten-fold higher level of CmAA7GT activity was found for anthocyanidin 3-*O*-rutinoside compared to anthocyanidin 3-*O*-monoglycosides (Table 2). In contrast, DgAA7GT utilizes cyanidin 3-*O*-glucoside, cyanidin 3-*O*-rutinoside, delphinidin 3-*O*-glucoside and delphinidin 3-*O*-rutinoside with almost identical efficiencies (Supplementary Table 2). Additionally, the glucosyltransferase activities of AaAA7GT toward anthocyanidin 3-*O*-monoglycosides are higher than toward anthocyanidin 3-*O*-rutinoside (Miyahara et al. 2012). The difference in acceptor preferences of CmAA7GT to those of DgAA7GT and AaAA7GT might possibly result from structural differences in their respective binding pockets for recognition of acceptor molecules. To date, analyses of GH1 enzyme crystal structures have shown that two glutamic acids act as the catalytic residues for glycoside hydrolase activity (Barrett

Table 2. Acceptor preferences of recombinant CmAA7GT.

Substrates	Relative activity (%)
Cyanidin	ND
Cyanidin 3-*O*-glucoside	10.3±0.7
Cyanidin 3-*O*-galactoside	3.6±0.1
Cyanidin 3-*O*-rutinoside	100.0±4.3
Cyanidin 3,5-*O*-diglucoside	ND
Pelargonidin	ND
Pelargonidin 3-*O*-glucoside	26.2±1.1
Delphinidin	ND
Delphinidin 3-*O*-glucoside	7.8±0.5
Delphinidin 3-*O*-rutinoside	95.0±4.0
Kaempferol	ND
Kaempferol 3-*O*-glucoside	ND
Naringenin	ND
Apigenin	ND

Analyses of acceptor preferences were performed with pHBG as the donor. The amount of reaction product was calculated from the area of the HPLC chromatogram. Relative activity is shown in comparison to cyanidin 3-*O*-rutinoside which was arbitrarily set as 100%. ND, not detected. All values are means±SD of at least three independent determinations.

et al. 1995; Burmeister et al. 1997; Chuenchor et al. 2011; Czjzek et al. 2000; Gloster et al. 2004; Sanz-Aparicio et al. 1998; Verdoucq et al. 2004). Although AAGTs show a ten times higher glucosyltransfer activity than glucoside hydrolase activity (Matsuba et al. 2010), these two catalytic glutamic acids are nevertheless conserved in AAGTs and in CmAA7GT (Supplementary Figure 3 asterisks). Determination of the structures of AAGTs and mutational studies based on such structural analyses will undoubtedly clarify the glucosyltransfer reaction mechanism and the motifs important for substrate recognition.

Acknowledgements

This work was supported by Grant-in-Aid for Scientific Research (B) (23370016) to Y.O., and Research Fellowships of Japan Society for the Promotion of Science for Young Scientists to Y.N.

References

Barrett T, Suresh CG, Tolley SP, Dodson EJ, Hughes MA (1995) The crystal structure of a cyanogenic β-glucosidase from white clover, a family 1 glycosyl hydrolase. *Structure* 3: 951–960

Burmeister WP, Cottaz S, Driguez H, Iori R, Palmieri S, Henrissat B (1997) The crystal structures of *Sinapis alba* myrosinase and a covalent glycosyl-enzyme intermediate provide insights into the substrate recognition and active-site machinery of an *S*-glycosidase. *Structure* 5: 663–675

Chuenchor W, Pengthaisong S, Robinson RC, Yuvaniyama J, Svasti J, Ketudat Cairns JR (2011) The structural basis of oligosaccharide binding by rice BGlu1 beta-glucosidase. *J Struct Biol* 173: 169–179

Czjzek M, Cicek M, Zamboni V, Bevan DR, Henrissat B, Esen A (2000) The mechanism of substrate (aglycone) specificity in β-glucosidases is revealed by crystal structures of mutant maize β-glucosidase-DIMBOA, -DIMBOAGlc, and -dhurrin complexes. *Proc Natl Acad Sci USA* 97: 13555–13560

Gloster TM, Macdonald JM, Tarling CA, Stick RV, Withers SG, Davies GJ (2004) Structural, thermodynamic, and kinetic analyses of tetrahydroozazine-derived inhibitors bound to β-glucosidases. *J Biol Chem* 279: 29236–49242

Honda T, Saito N (2002) Recent progress in the chemistry of polyacylated anthocyanins as flower color pigments. *Heterocycles* 56: 633–692

Kondo T, Oki K, Yoshida K, Goto T (1990) Structure of violdelphin, an anthocyanin from violet flower of *Delphinium hybridum*. *Chem Lett* 19: 137–138

Matsuba Y, Sasaki N, Tera M, Okamura M, Abe Y, Okamoto E, Nakamura H, Funabashi H, Takatsu M, Saito M, et al. (2010) A novel glucosylation reaction on anthocyanins catalyzed by acyl-glucose-dependent glucosyltransferase in the petals of carnation and delphinium. *Plant Cell* 22: 3374–3389

Miyahara T, Takahashi M, Ozeki Y, Sasaki N (2012) Isolation of an acyl-glucose-dependent anthocyanin 7-*O*-glucosyltransferase from the monocot *Agapanthus africanus*. *J Plant Physiol* 169: 1321–1326

Miyahara T, Sakiyama R, Ozeki Y, Sasaki N (2013) Acyl-glucose-dependent glucosyltransferase catalyzes the final step of anthocyanin formation in Arabidopsis. *J Plant Physiol* 170: 619–624

Nishizaki Y, Yasunaga M, Okamoto E, Okamoto M, Hirose Y, Yamaguchi M, Ozeki Y, Sasaki N (2013) *p*-Hydroxybenzoyl-glucose is a Zwitter donor for the biosynthesis of 7-polyacylated anthocyanin in delphinium. *Plant Cell* 25: 4150–4165

Sanz-Aparicio J, Hermoso JA, Martínez-Ripoll M, Lequerica JL, Polaina J (1998) Crystal structure of β-glucosidase A from *Bacillus polymyxa*: Insights into the catalytic activity in family 1 glycosyl hydrolases. *J Mol Biol* 275: 491–502

Saito N, Tatsuzawa F, Yazaki Y, Shigihara A, Honda T (2007) 7-Polyacylated delphinidin 3,7-diglucosides from the blue flowers of *Leschenaultia* cv. Violet Lena. *Phytochemistry* 68: 673–679

Terahara N, Toki K, Saito N, Honda T, Isono T, Furumoto H, Kontani Y (1990) Structures of campanin and rubrocampanin, two novel acylated anthocyanins with *p*-hydroxybenzoic acid from the flowers of bellflower, *Campanula medium* L. *J Chem Soc Perkin Trans* 1: 3327–3332

The Angiosperm Phylogeny Group (2009) An update of the Angiosperm Phylogeny Group classification for the orders and families of flowering plants: APG III. *Bot J Linn Soc* 161: 105–121

Verdoucq L, Morinière J, Bevan DR, Esen A, Vasella A, Henrissat B, Czjze M (2004) Structural determinants of substrate specificity in family 1 β-glucosidases: Novel insights from the crystal structure of sorghum dhurrinase-1, a plant β-glucosidase with strict specificity, in complex with its natural substrate. *J Biol Chem* 279: 31796–31803

Yonekura-Sakakibara K, Nakayama T, Yamazaki M, Saito K (2009) Modification and stabilization of anthocyanins. In: Gould K, Davis K, Winefield C (eds) *Anthocyanins Biosynthesis, Functions, and Applications*. Springer Science+Business Media, pp 170–190

Yoshida K, Mori M, Kondo T (2009) Blue flower color development by anthocyanins: from chemical structure to cell physiology. *Nat Prod Rep* 26: 884–915

Supplementary Table 1

Oligonucleotide primer sequences

Primer name	Sequence (5' to 3')
AAGTdgF	TGYTTYMRNRANTAYGGNGA
AAGTdgR	GCRTGNGCGNARNARNADNAVRTGRTG
Cm7GT5'raceR	TATAGCCTTGCAGTTGATGCATGTGCC
Cm7GTatgF	ATGTTGACCCAAAACCAATTAAAATG
Cm7GTstpR	TCATGAAGAAGCTGAACTCTT
Cm7GTexpF	ATGGATTATAGCAGACTTG
Cm7GTrtR	TGAAGAAGCTGAACTCTT
Cm7GTF	CGCGGGAACTTCCGCTTATCA
Cm7GTR	TATCTGCATTGGCTCCGCCT
CmEF1aF	GGTGGTCTCAAACTTCCACAAGGCA
CmEF1aR	TCATTCAAGTATGCCTGGGTGTTGG

Supplementary Table 2

Acceptor preference of DgAA7GT

Substrates	Relative activity (%)
Cyanidin 3-*O*-glucoside	98.5 ± 0.9
Cyanidin 3-*O*-rutinoside	100.0 ± 0.0
Delphinidin 3-*O*-glucoside	82.2 ± 0.8
Delphinidin 3-*O*-rutinoside	76.1 ± 2.7

Analyses of acceptor preferences were performed with pHBG as the donor. The recombinant DgAA7GT protein (Matsuba et al. 2010) was prepared and the enzyme reaction for DgAA7GT was performed in the same constituent reaction mixture and the incubation condition as that for CmAA7GT described in the manuscript. The amount of reaction product was calculated from the area of the HPLC chromatogram recorded at 530 nm. Relative activity is shown in comparison to cyanidin 3-*O*-rutinoside which was arbitrarily set as 100%. All values are means ± SD of at least three independent determinations.

Supplementary Figure 1

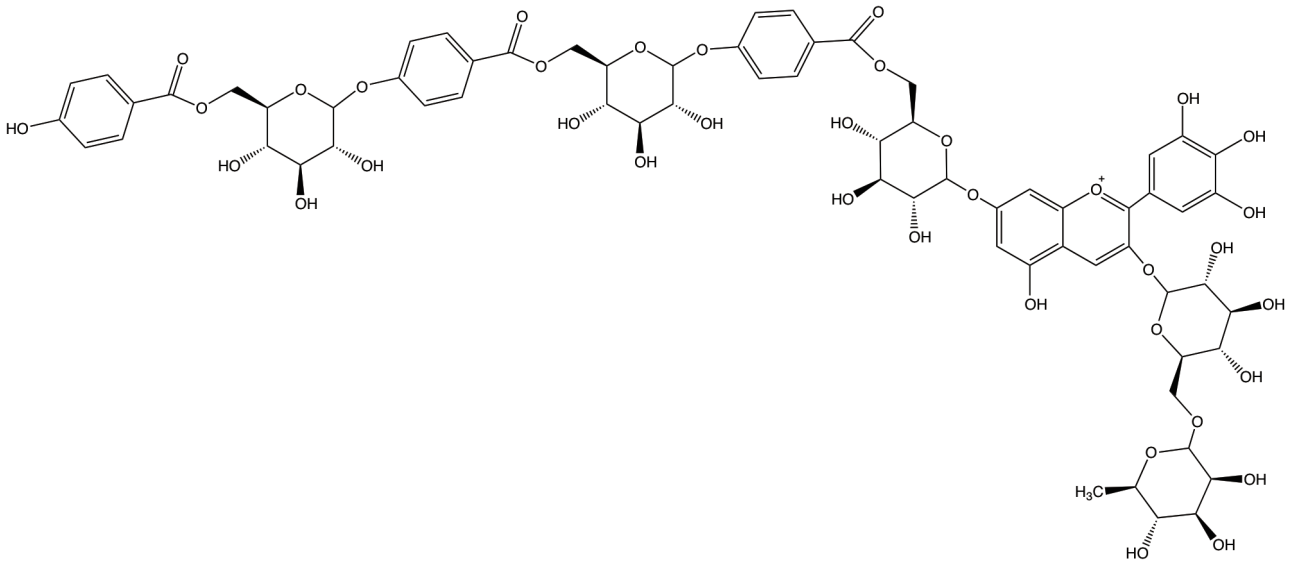

Supplementary Figure 1. The anthocyanin structure present in *C. medium* petals.

Supplementary Figure 2

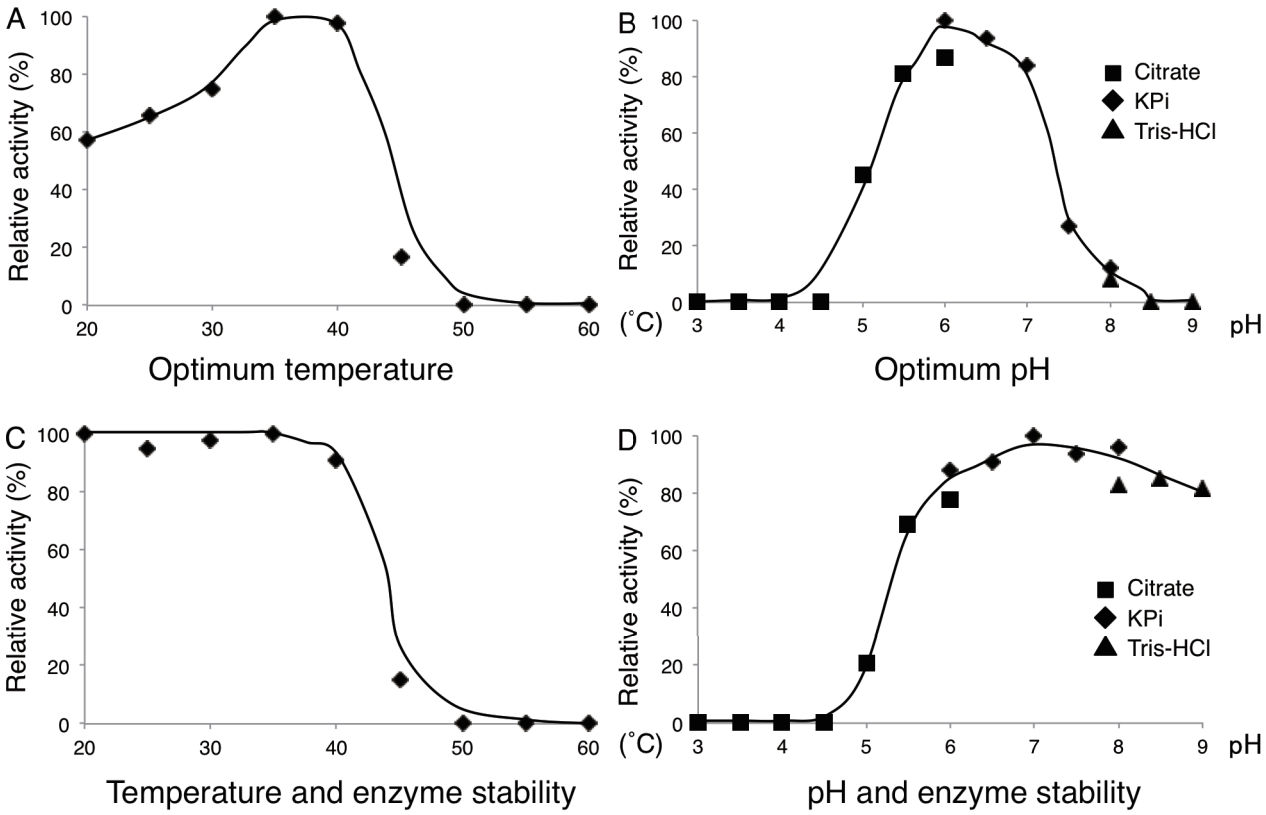

Supplementary Figure 2. Partial enzymatic properties of recombinant CmAA7GT protein. (A) The optimum reaction temperature for activity at pH 6.0 in potassium phosphate buffer. (B) The optimum reaction pH for enzyme activity. (C) Thermostability of the enzyme in potassium phosphate buffer at pH 6.0. (D) Stability of the enzyme at different pHs. Closed squares, sodium citrate buffer; closed diamond, potassium phosphate buffer; closed triangle, Tris-HCl buffer.

Supplementary Figure 3

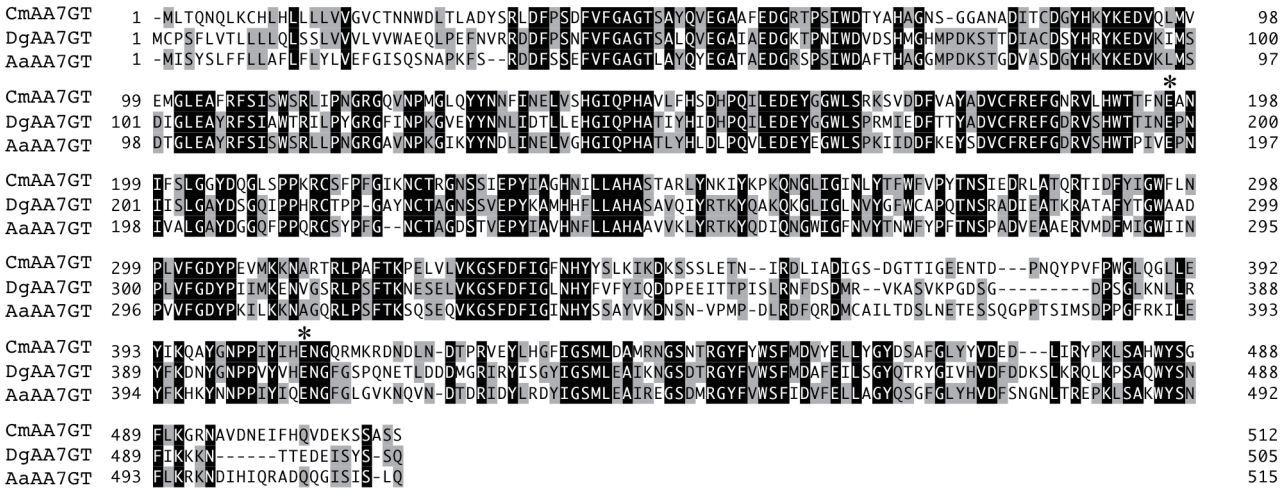

Supplementary Figure 3. Alignment of AA7GTs amino acid sequences.

Identical residues are shaded in black and similar ones in gray. The sequences were aligned using CLUSTALW. The two asterisks indicate catalytic glutamic acids that are highly conserved in GH1 proteins.